Electronic Structure and Stability of Binary and Ternary Aluminum-Bismuth-Nitrogen Nanoclusters

Alan Miralrio and Luis Enrique Sansores*

The electronic structure and stability in binary and ternary aluminum-bismuth-nitrogen nanoclusters up to six atoms are studied using density functional theory (DFT). The lowest energy geometries were obtained by sampling the geometrical space with a Monte Carlo method and geometry optimizations, at DFT level, with M06L functional. The clusters stability is analyzed using formation and fragmentation energies. Our results show that a high concentration of nitrogen presents a tendency to form nitrogen clusters. highest occupied molecular orbital-lowest unoccupied molecular orbital gaps show the well-known oscillation as the number of atoms is increased. Bonding between Al, Bi, and N has mainly a π character. Bismuth and aluminum atoms tend to promote high multiplicity states in small clusters. These new binary and ternary materials provide a potential new field in optoelectronics and high energetic material compounds. © 2014 Wiley Periodicals, Inc.

DOI: 10.1002/qua.24693

Introduction

Clusters are atomic or molecular aggregates bonded by different interactions with a defined number of constituents. Nanoclusters (with size in the nanoscale) are commonly formed by a core of heavy atoms with ligands of light atoms surrounding it. Its properties are strongly related to size, geometry, and number of constituents, opposed to the bulk material where size effects are negligible. Cluster's different physical and chemical properties open new possible applications with sizes comparable to most biological and electronic systems, and make them an important topic in today's research. Particularly, the interest in metallic clusters (formed by atoms that are metals in bulk) lays in the possibility of new properties (electronic, optic, magnetic, etc.), as their main interactions in bulk can be affected at nanoscale limit.

Properties of members of group 15 of the periodic table change through the group, from nonmetals (N, P), metalloids (As, Sb) up to Bi a heavy metal. This is consistent with a decrease in the covalent character of the bond and an increase in the metallic character. It is well-known the importance of nitrides in electronics, like aluminum nitride AlN. The combination of aluminum with other member of the nitrogen group, like bismuth, opens new possibilities. Research on nanoclusters of these elements is relevant as their electronic, optic, and magnetic properties can be mutually affected.

Aluminum nanoclusters, Al_n, have been synthesized[1,2] by laser ablation. The time of flight mass spectrometry shows[3] that Al_7^+, Al_{13}^-, and Al_{23}^- are stable, consistent with magic numbers of the spherical Jellium model, with 20, 40, and 70 electrons respectively.[4] In Stern-Gerlach experiments[1] the $Al_{n=odd}$ shows a magnetic moment, but even clusters like Al_4 and Al_2 show greater magnetic moments, due to their high multiplicity state. Al_{13}^- and Al_{20} also obey de Jellium shell closure rule and are considered as very stable.[5] Conversely, small aluminum clusters show odd–even alternations of various properties,[6] per example ionization potential and detachment energies.

Experimentally, nanoparticles of Bi are semimetallic rhombohedral clusters, similar to bulk, but have a transition phase to amorphous semiconductor below 1300 atoms.[7–9] Bi_n nanoclusters synthesized in gas state by laser ablation show that Bi_3^+, Bi_5^+, and Bi_7^+ are stable in mass spectrometry studies.[10] Theoretical density functional theory (DFT) studies of $Bi_{n=2-24}$ clusters show[11] that geometries are formed by boxes with pentagonal faces. The synthesized cations $Bi_{n=4-14}^+$ present similar structures in ion trapped electron diffraction studies.[12] Clusters have important even–odd alternations in their energies,[11] giving relative stability in $Bi_{n=even}$ and $Bi_{n=odd}^+$ with greater highest occupied molecular orbital (HOMO)-lowest unoccupied molecular orbital (LUMO) gaps. Even–odd oscillations decrease while the number of atoms increases. Above 20 atoms Bi_n shows HOMO-LUMO gaps around 1.6 eV as expected for a semiconductor. In Stern–Gerlach experiments the $Bi_{n=odd}$ clusters show paramagnetic deflections[13]; Measured magnetic moments are greater than the theoretical values.[11] This is explained by the spin-orbit interaction[8] not taken into account in those studies. Recently, Bi clusters in the range size 0.5–1.4 nm studied by photoelectron spectroscopy[14] show a metallic behavior with structures similar to polycrystalline Bi.[14]

High natural stability of N_2 hinders the formation of other forms of nitrogen, azide N_3^- a well-known nucleophile, forms covalent and ionic bonds with metals. These compounds are commonly toxic, when used in biochemistry in mutagenesis[15] and explosive when mixed with metals.[16] They also have

A. Miralrio, L. E. Sansores
Departamento de Materiales de Dimensionalidad Restringida, Instituto de Investigaciones en Materiales, Universidad Nacional Autónoma de México, Apartado, Postal 70-360, México, DF 04510, México
E-mail: sansores@unam.mx

Table 1. Comparison between experimental and theoretical bond lengths (Å).

Method	Bond length (Å)	Error (%)
Bi_2		
Experimental [36]	2.66	
MCSCF [37]	2.84	6.77
M06-L/LANL2DZdp	2.59	−2.63
Bi_2^+		
Experimental [36]	2.86	
MCSCF [37]	3.01	5.24
M06-L/LANL2DZdp	2.70	−5.59

other applications, like the sodium azide in airbags for automobiles. More recently, cation N_5^+ was synthesized,[17] with a planar structure with symmetry C_{2v},[18] it is stable up to 20°C in solid form. Finally, the N_5^- has been detected in mass spectrometry signals.[19] Theoretical studies agree with these results, which have been performed at MP2 (FU)/6-31G(d) level of theory.[18] The most stable N_5 isomer is a weak N_2—N_3 complex.

Aluminum nitride, AlN, is a well-known semiconductor with wide band gap of 6.2 eV and possible applications in ultraviolet optoelectronics.[20] Nanoscopic clusters Al_nN_m synthesized by laser ablation show that AlN, Al_2N, AlN_3, and Al_4N_2 are stable.[21] Theoretical calculations and time of flight experiments show that in small clusters they form linear and bidimensional structures with no transition to tridimensional geometries.[22,23] The relative stability of these clusters can be related with the N—N bonds according to theoretical work.[22] Another work,[24] shows that Al_3N and Al_5N are stable. According to the Jellium model Al_5N is the first cluster with a completely closed shell with 20 valence electrons. Recently[25] the production of anionic and cationic Al_n, Al_nN_m, and N_n clusters via laser ablation in AlN nanopowder open the possibility to obtain other binary (or ternary) clusters with nitrogen.

Binary Al_nBi_m clusters have been synthesized in gas phase by laser ablation[26,27]; Al_3Bi and Al_5Bi are found stable in experiments and theoretical studies.[26] Results from theoretical study are consistent with aromatic stability in planar Al_3Bi and Jellium stability in Al_5Bi. The DFT method used is PBE96 functional with the DZVP basis for Al, and a 23 electron ECP with aug-cc-pVDZ basis for Bi.[26] Time of flight experiments and theoretical results, at DFT level, show that $Al_2Bi_3^-$ is especially stable[27] within the series $(Al_{n=1-12} Bi_{m=1-4})^-$. These calculations have been performed with B3LYP functional and 6-311+G(3df) basis for Al and relativistic effective core potential basis LANL2DZdp for Bi.

Finally, synthesis of binary bismuth-nitrogen compounds, $Bi(N_3)_3$, $[Bi(N_3)_4]^-$, and $[Bi(N_3)_6]^{3-}$, has been reported.[28] The geometry of bismuth three azide, found by the same group, shows a central Bi with a helix of azide and symmetry C_3; this structure was found in a DFT study with B3LYP functional, 6-31G(d) basis for N and ECP78MWB quasirelativistic pseudopotential for Bi. The other two, have been synthesized in salts,[28] showing networks of nitrogen around a single Bi atom; More recently, the synthesis of the $Bi(N_3)_3$ in purified form has been reported[29] by the same group.

In this article, we study $Al_xBi_yN_z$ nanoclusters where $x + y + z \leq 6$ searching for the stable lowest energy geometries using DFT. The stability of clusters is analyzed using formation and fragmentation energies. Also electronic, magnetic, and geometric properties are studied.

Computational Methods

For each stoichiometry, several stable geometries can exist, each one is a local minimum in the potential energy surface; in this work we searched for the global minima using a simple Monte Carlo method[30,31] and followed by optimizations with DFT using Gaussian 09.[32] Final optimizations were done using the mega-GGA functional M06-L of Truhlar and Zhao.[33] This functional is adjusted to work with main group elements, transition metals, thermochemistry, and non-covalent interactions. It has been adjusted to 314 experimental data, and compared with other 11 functionals showing the best results in the above fields. The basis used for Al and N was 6-311+G(3df) that adds polarization functions by three sets of d and one f functions and a set of diffusive sp functions.[34,35] For bismuth, the heavy nature of this element requires the use of pseudopotentials to model the inner electrons. We have used the LANL2DZdp basis; this is a scalar relativistic pseudopotential that considers 78 core electrons, with a double zeta set for valence orbitals.

To test our chosen DFT functional and Bi basis, we calculated the bond length of Bi_2 and Bi_2^+ with M06-L and LANL2DZdp and compare with experimental results and previous theoretical calculations. Table 1 shows the bond length obtained and errors respect to the experimental results. Our error is smaller for the neutral binary and slightly bigger for the cation.

Basis set 6-311+G has been used previously in calculations of electronic structure for $Al_nAs_m^-$ clusters[38,39] and together with the LANL2DZdp basis for Bi in calculations of vertical detachment energies (VDE) and binding energies[40] of anionic Bi_nGe_m, Bi_nSi_m, Bi_nSn_m, and binding energies[27] of Al_nBi_m, clusters. These theoretical results agree well with the experimental results.[27,38–40]

Method M06-L/6-311+G(3df)/LANL2DZdp agrees well with experimental bond lengths of Al_2[41] and N_2[42] and with the theoretical result[26] for AlBi (Table 2). The errors obtained −1.11, −0.08, and 0.02%, respectively, are smaller than those obtained with smaller basis 6-31G(d) for Al and N.

Table 2. Comparison between experimental and theoretical bond lengths of Al_2 (Triplet), N_2 (Singlet), and AlBi (Triplet).

	Bond length relative error (%)		
Method/Cluster	Al_2(T) [41]	N_2(S) [42]	AlBi(T) [26]
B3LYP/6-31G(d)	1.76	0.68	1.86
M06-L/6-31G(d)	−1.05	1.11	0.14
PBE96/6-31G(d)	1.08	1.71	1.5
B3LYP/6-311+G(3df)	1.31	−0.65	1.55
M06-L/6-311+G(3df)	−1.11	−0.08	0.02
PBE96/6-311+G(3df)	0.77	0.42	11.06

Table 3. Comparison of the calculated errors respect the experimental VDE of $Al_{n\,=\,1-5}Bi$.

Method/Cluster	VDE relative error (%)					Total error (%) $Al_{n=1-5}Bi$
	AlBi	Al_2Bi	Al_3Bi	Al_4Bi	Al_5Bi	
M06-L/6-31G(d)/LANL2DZdp	2.80	−4.22	−20.48	4.93	−2.31	10.00
M06-L/6-31+G(3df)/LANL2DZdp	9.20	−5.06	−7.62	5.38	0.38	7.00
M06-L/6-311+G(3df)/LANL2DZdp	4.00	−8.02	−14.29	2.24	−6.54	7.58
PBE96/6-311+G(3df)/LANL2DZdp	20.80	−3.80	−8.57	6.73	−1.92	11.55
PBE96/DZVP/ECP(Bi) [26]	8.00	−2.11	−7.14	8.52	0.00	6.73

We also calculated the VDE of $Al_{n\,=\,1-5}Bi$ with M06-L using basis sets 6-31G(d), 6-31+G(3df), and 6-311+G(3df) for Al and LANL2DZdp for Bi. We also calculated VDE with PBE96 and 6-311+G(3df)/LANL2DZdp. To calculate the VDE, we optimized anions $Al_{n1-5}Bi^-$ to a global minimum, the VDE's are calculated as the energy difference between the neutral, with the geometry of the optimized anion, and the anion (according with a vertical transition). Table 3, shows the relative error between the experimental VDE[26] for each cluster and the corresponding method. The total error was taken as the standard deviation for each method. The smallest error is 6.73% for PBE96/DZVP/ECP(Bi),[26] followed by the M06-L/6-31+G(3df)/LANL2DZdp with 7 and 7.58% for M06-L/6-311+G(3df)/LANL2DZdp.

In conclusion, method M06-L/6-311+G(3df)/LANL2DZdp gives the best bond lengths while the VDE errors are similar to those of PBE96/DZVP/ECP(Bi). Our final calculations were done using M06-L/6-311+G(3df)/LANL2DZdp, as this method shows a good performance in geometries and reasonable VDEs; conversely, the basis sets were used before in other works of aluminum, bismuth, and binaries clusters[27,38–40] and allows us to do comparisons.

All the geometries presented in this work have real vibrational frequencies and are to the best of our knowledge the lowest local minima. The lowest energy geometry was also optimized increasing the multiplicity until a geometry with higher energy was found. The geometry with the lowest energy is considered the global minimum. To validate the Monte Carlo + DFT method, we compared the results of global optimization applied for pure clusters $Al_{n\,=\,2-6}$, $Bi_{n\,=\,2-6}$, and $N_{n\,=\,2-6}$. Geometries, multiplicities, and symmetries obtained are shown in Figure A (Supporting Information). The Bi_n geometries agree well with those reported,[11] showing the transition to three-dimensional (3D) structures for $Bi_{n\,>\,3}$. The aluminum clusters Al_n agree with previous calculations[4,43] except for Al_5 of Ref. [4]. Our result shows a flat geometry with symmetry C_{2v} in agreement with Ref. [43]. Finally, for nitrogen clusters, N_n, we reproduce its known behavior, forming a lineal N_3 similar to the azide, and the N_5 is an aggregate[18] of N_3 and N_2. The C_{2v} structure for N_6 is very unstable.

Results and discussion

Binary and ternary clusters

Figure 1 shows the lowest energy geometries for binary clusters Al_xBi_y with its multiplicity and symmetry. Several binary clusters show physical substitutions, interchanging one atom
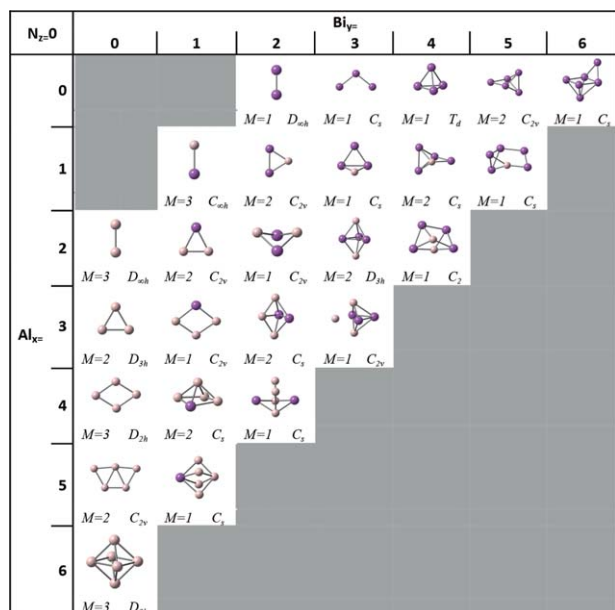

Figure 1. Lowest energy geometries of Al_xBi_y. In the lower part of each cell the multiplicity and group symmetry are indicated. [Color figure can be viewed in the online issue, which is available at wileyonlinelibrary.com.]
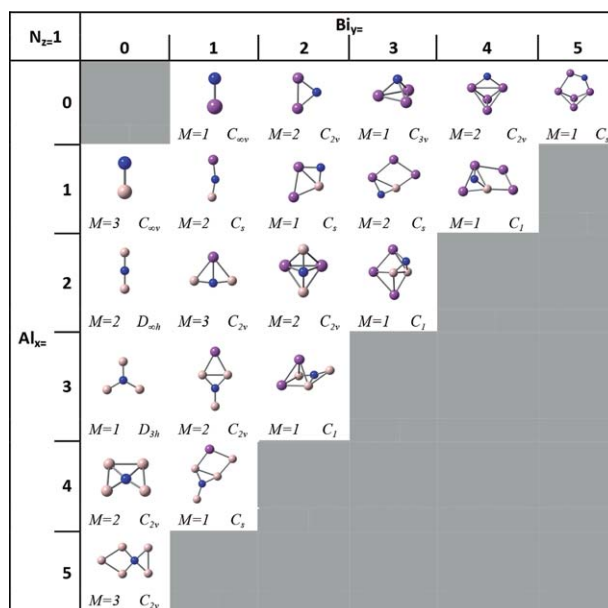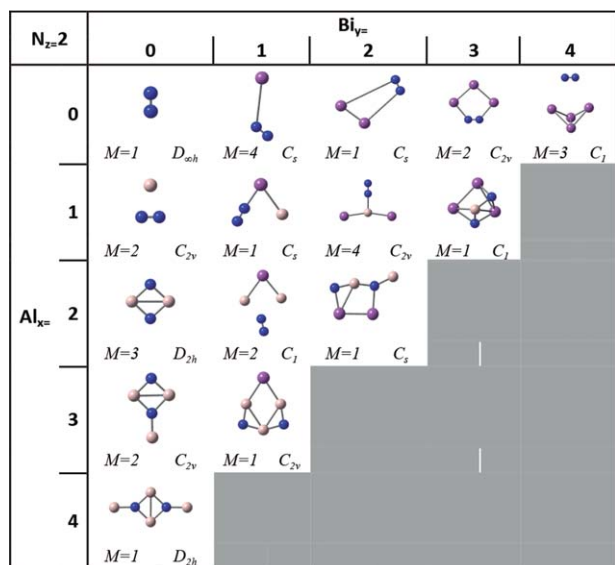

Figure 2. Lowest energy geometries of Al_xBi_yN. In the lower part of each cell the multiplicity and group symmetry are indicated. [Color figure can be viewed in the online issue, which is available at wileyonlinelibrary.com.]
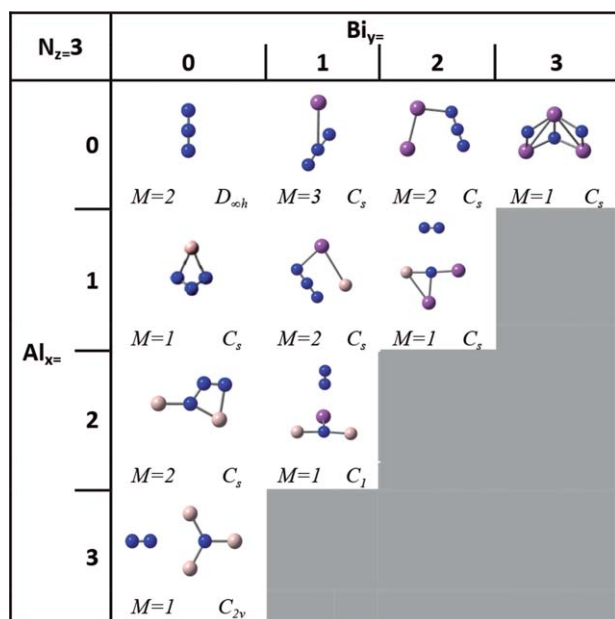
Figure 3. Lowest energy geometries of $Al_xBi_yN_2$. In the lower part of each cell the multiplicity and group symmetry are indicated. [Color figure can be viewed in the online issue, which is available at wileyonlinelibrary.com.]

Figure 5. Lowest energy geometries of $Al_xBi_yN_4$. In the lower part of each cell the multiplicity and group symmetry are indicated. [Color figure can be viewed in the online issue, which is available at wileyonlinelibrary.com.]
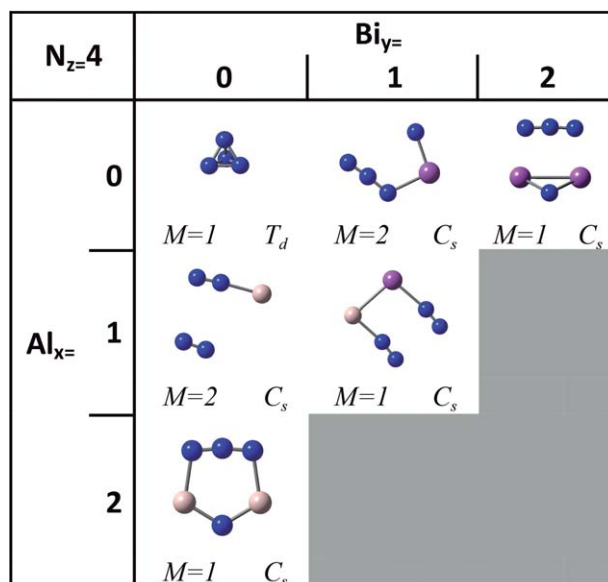
by another in the structure. Al_n cluster shows a flat structure and Bi_n has 3D structures. As we substitute Al atoms by Bi, the structure evolves to be 3D, every time more similar to the 3D Bi_n structure. For example, in Al_3 and Al_4 clusters, with symmetries D_{3h} and D_{2h}, respectively, successive substitutions up to Bi_3 and Bi_4 transforms to C_{2v} and T_d symmetries, respectively. The p orbitals available in bismuth tend to modify the bond angles, these orbitals cannot form an sp^2 hybridization by the inert pair effect, so these orbitals can only form bonds with angles around $90°$ similar to angles between pure p orbitals. The obtained Al_xBi geometries agree well with those

reported,[26] the only exception is Al_4Bi[26] reported like a planar geometry, similar to Al_5 but with a central Bi. In our calculations, the same geometry shows imaginary vibrational frequencies; our stable geometry was a distorted pyramid.

The obtained geometries are presented by increasing nitrogen content series. Optimized geometries, for the first series, with only one nitrogen, Al_xBi_yN, are shown in Figure 2. They show similar physical substitutions, as previously mentioned for clusters without N. The binary Al_xN clusters have planar geometries, with some substitutions in the pure aluminum clusters. The tendency to form planar structure was reported previously.[21,22] Our geometries are in agreement with other calculations,[24] except Al_5N, obtained as a triplet C_{2v}, with a
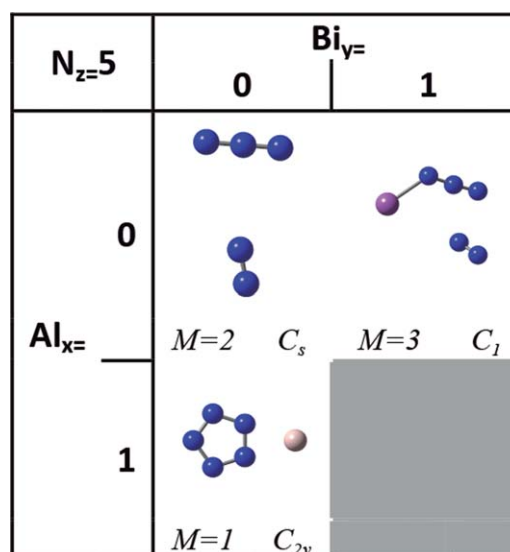

Figure 4. Lowest energy geometries of $Al_xBi_yN_3$. In the lower part of each cell the multiplicity and group symmetry are indicated. [Color figure can be viewed in the online issue, which is available at wileyonlinelibrary.com.]
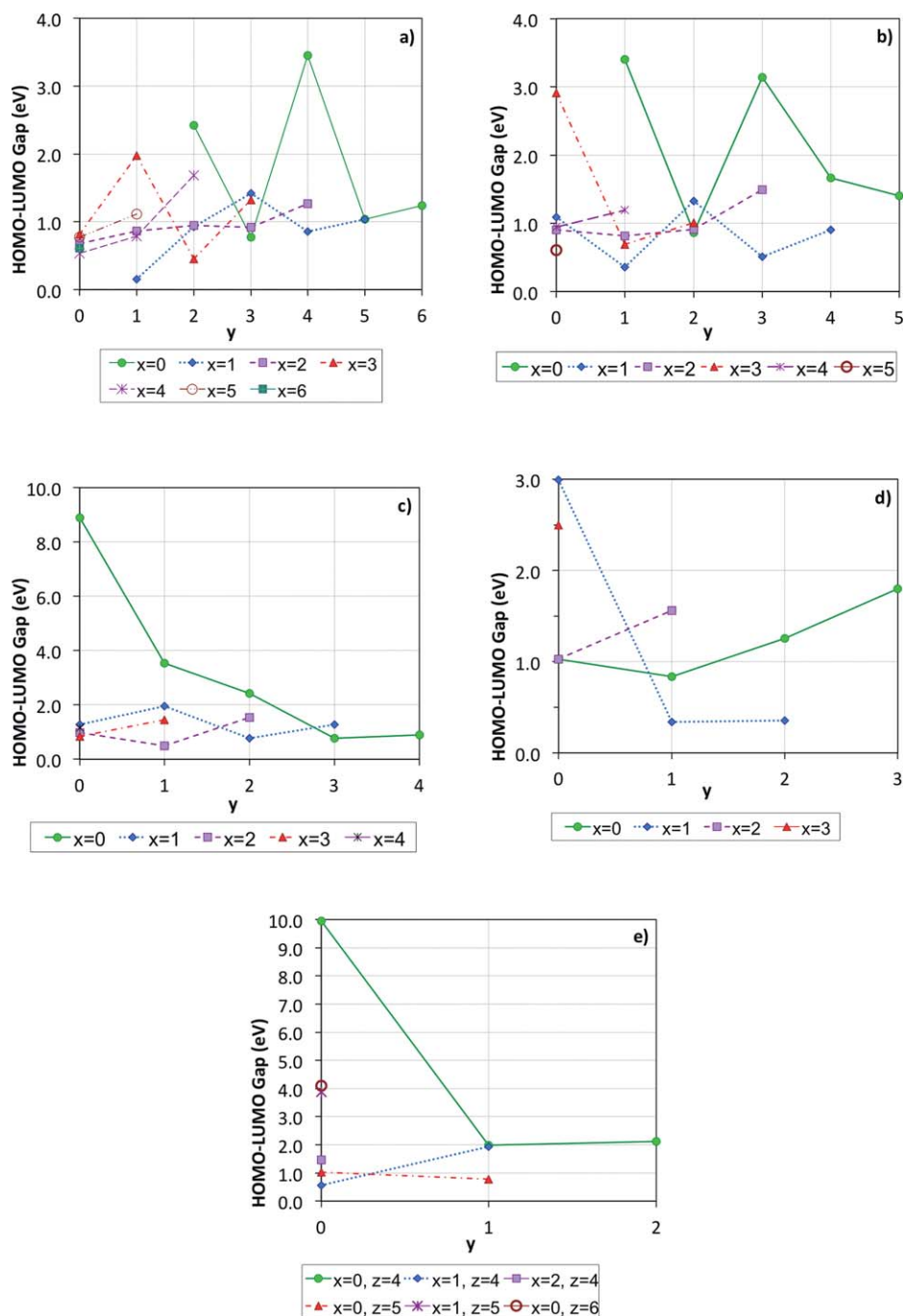

Figure 6. Lowest energy geometries of $Al_xBi_yN_5$. In the lower part of each cell the multiplicity and group symmetry are indicated. [Color figure can be viewed in the online issue, which is available at wileyonlinelibrary.com.]

Figure 7. HOMO-LUMO gap as a function of Bi concentration (y) for $Al_xBi_yN_z$. a) Without nitrogen, b) nitrogen concentration=1 ($z = 1$), c) nitrogen concentration=2 ($z = 2$), d) nitrogen concentration=3 ($z = 3$), and e) nitrogen concentration=4 and 5 ($z = 4$ and $z = 5$). [Color figure can be viewed in the online issue, which is available at wileyonlinelibrary.com.]

nonplanar structure similar to our Bi_5. This structure is in agreement with Ref. [23]. The atomic substitutions do not necessarily change the planarity, for example, the nitrogen and bismuth substitutions between Al_3Bi, Al_2BiN, and $AlBi_2N$ preserve the planarity. This is result of the available p orbitals perpendicular to the atomic plane and the sp^2 hybridization in N and Al. Conversely, clusters containing four or more bismuth atoms show 3D geometries. Ternary clusters Al_3BiN, Al_2BiN, $AlBi_3N$, and Al_4BiN show planar geometries, due to the avail-

able pure p orbitals. In binary Bi_yN clusters, this behavior tends to form 3D structures with the N bonded between two or more bismuths.

Adding a second nitrogen atom, we obtained the second series with geometries shown in Figure 3. High stability of nitrogen molecule hinders the formation of mixed structures, especially in clusters containing bismuth (BiN_2, Bi_2N_2, and Al_2BiN_2). These clusters show nitrogen dimers around the Bi. Conversely, aluminum-nitrogen clusters like Al_2N_2, Al_3N_2, and
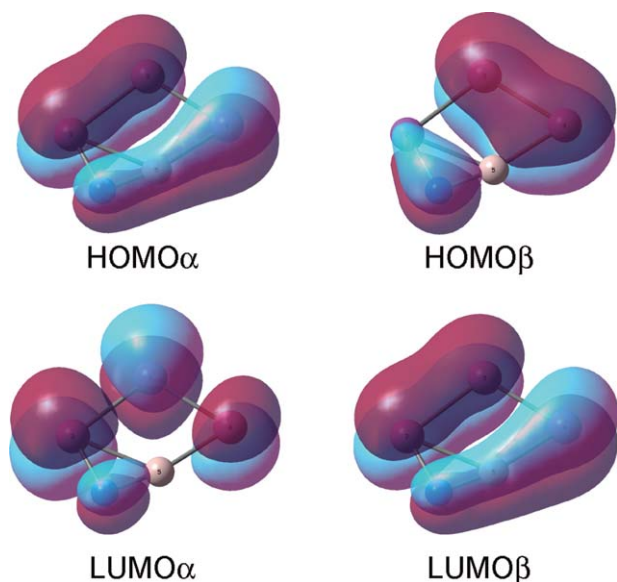
Figure 8. Spatial representation of HOMO and LUMO of $AlBi_3N$. [Color figure can be viewed in the online issue, which is available at wileyonlinelibrary. com.]

Al_4N_2 show planar structures and nitrogen's do not form dimers.

Figure 4 shows optimized structures of the next series with three nitrogen atoms. Nitrogen trimer appears like a ligand azide N_3^- mainly around bismuth atoms, indicating some bonding preference with Bi. This behavior has been reported previously in the synthesized binary compounds of bismuth-nitrogen, the BiN_3 is an example.[28] The known behavior of azide as a ligand in presence of metals is different with aluminum; also in Al_xN_3 nitrogen clusters tend to form trimers around aluminum atoms. Bi_3N_3 shows a C_s structure similar to N_6 with the substitution of three Bi atoms. Notable exceptions are Al_3N_3, Al_2BiN_3, and $AlBi_2N_3$, showing a N_2 dimer weakly bonded around a structure with a central N. For the last two clusters bond lengths to the dimer are 2.544 and 3.277 Å, respectively.

With four nitrogen atoms, we obtained the geometries shown in Figure 5. The N_4 structure was obtained as a tetrahedral cluster reported experimentally[44] as unstable, with a lifetime of microseconds. The BiN_4 shows a similar behavior to
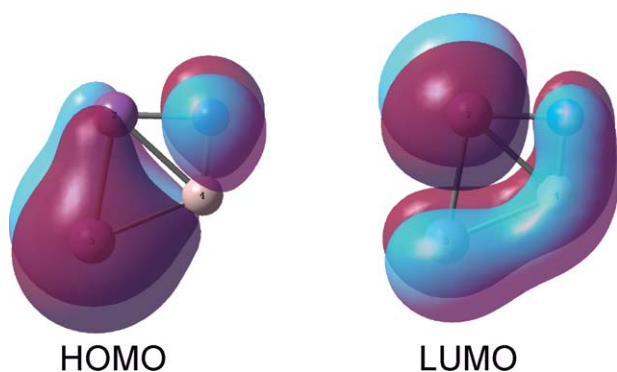

Figure 9. Spatial representation of HOMO and LUMO of $AlBi_2N$. [Color figure can be viewed in the online issue, which is available at wileyonlinelibrary. com.]
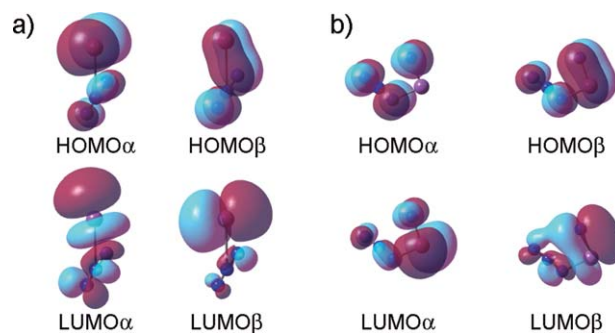

Figure 10. Spatial representation of HOMO and LUMO: a) BiN_3 and b) BiN_4. [Color figure can be viewed in the online issue, which is available at wileyonlinelibrary.com.]

BiN_3, with the Bi—N bonded to an N_3. Also N_3 trimer is present in Bi_2N_4 and Al_2N_4. This is due to the high stability of the azide and low stability of the N_4.

Finally, with five nitrogen atoms, AlN_5 is formed by a nitrogen pentamer and a weakly bonded Al (Fig. 6). In this case, N_5 is stabilized by donation of an electron from Al. The bond length between the ring and the Al is 2.073Å. The pentamer N_5 corresponds to a trimer weakly bonded to a dimer, this has been seen before in theoretical works.[18]

HOMO-LUMO orbitals

To analyze the electronic properties, we calculated the HOMO and the LUMO. For open shell systems, we calculated the HOMOα, HOMOβ, LUMOβ, and LUMOβ according to the spin. We used the open shell HOMO-LUMO gap defined by

$$E_{\sigma\sigma'} = |E(\text{HOMO}_{\sigma'}) - E(\text{LUMO}_\sigma)| \, \sigma, \sigma' = \alpha, \beta$$
$$E_{\text{HOMO-LUMO}} = \min\{E_{\sigma\sigma'}\} \tag{1}$$

For a global analysis of all obtained $Al_xBi_yN_z$ clusters, we present the HOMO-LUMO gaps in Figure 7 in terms of groups with the same number of nitrogen concentration (Energies values of the gap, HOMO and LUMO are given in Table A of the Supporting Information). The known oscillation of the gap reported for pure bismuth clusters[11] are reproduced in our work. These oscillations are due to the closed shell effect on the even-atom clusters. A closed shell requires more energy to extract electrons from the cluster, then the HOMO-LUMO gap of even-atom cluster are much higher compared with the odd-atom cluster; for example, in Figure 7a the odd-atom clusters Bi_3 and Bi_5 with gaps of 0.774 and 1.034 eV, respectively, have lower gap energies than the even-atom clusters Bi_2, Bi_4, and Bi_6 with 2.425, 3.449, and 1.241 eV, respectively. The same behavior is observed in binary series $Al_3Bi_{y=0-3}$ and $AlBi_{y=2-5}$. Also in Figures 7b and 7c the binary series $Bi_{y=1-4}N$ and ternary $AlBi_{y=0-4}N$ $AlBi_{y=0-3}N_2$ show even–odd oscillations. Conversely, series $Al_2Bi_{y=2-4}$, $Bi_{y=0-4}N_2$, $Al_2Bi_{y=0-3}N$, and $Bi_{y=0-3}N_3$ (Figures 7a, 7c, and 7d) have a monotonic behavior. In the first three cases this is probably due to the pairing of the electrons of Al_2 and N_2; the last one has a small oscillation around BiN_3.
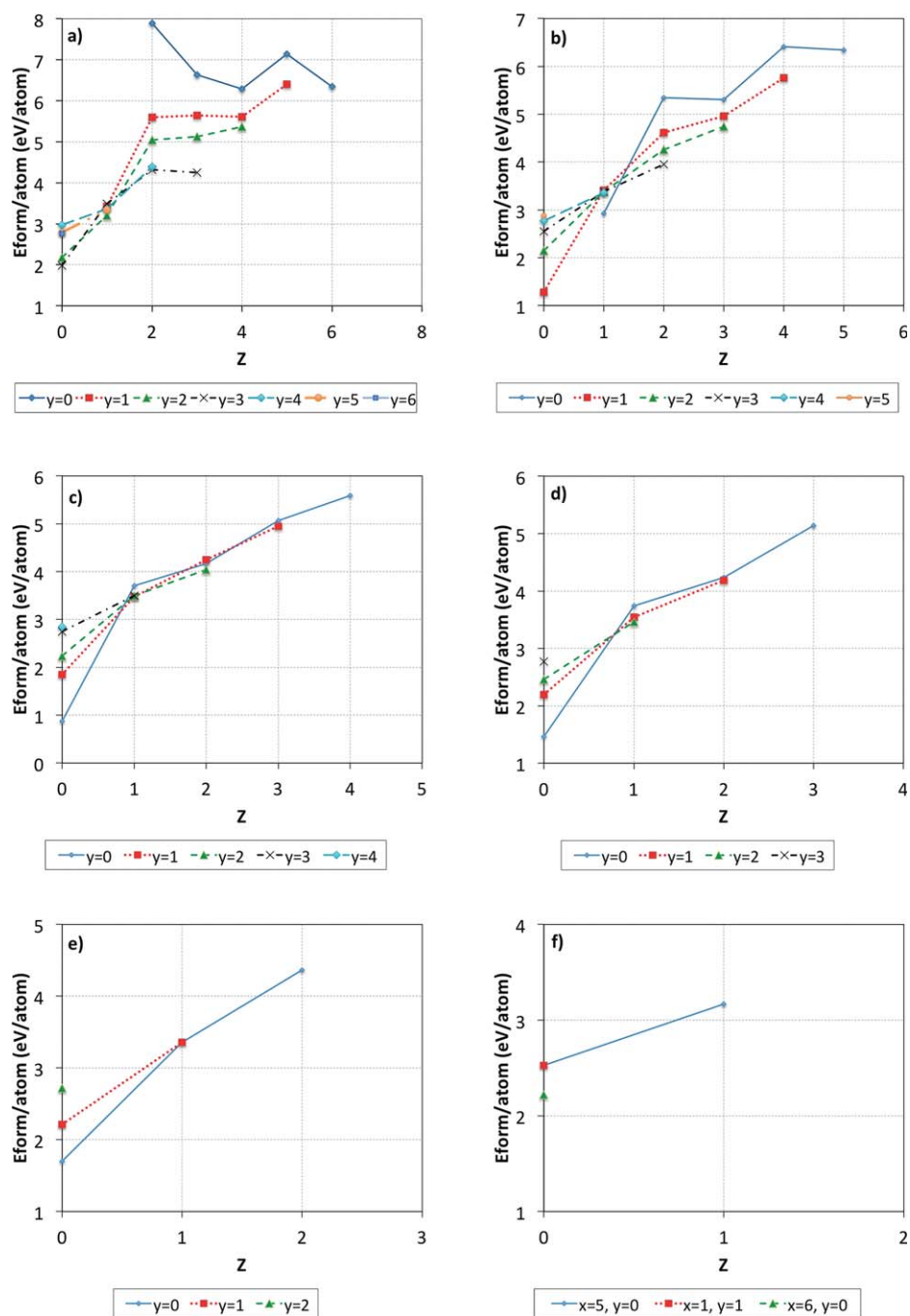
Figure 11. Formation energy per atom as a function of nitrogen concentration (z) for $Al_xBi_yN_z$. a) Witout Al ($x = 0$), b) aluminum concentration=1 ($x = 1$), c) aluminum concentration=2 ($x = 2$), d) aluminum concentration=3 ($x = 3$), e) aluminum concentration=4 ($x = 4$), and e) aluminum concentration=5 and 6 ($x = 5$ and $x = 6$). [Color figure can be viewed in the online issue, which is available at wileyonlinelibrary.com.]

Most ternary clusters $Al_xBi_yN_z$ have gaps below 1.6 eV; this can be understood by their planar structures since the p orbitals may have formed bonding π orbitals extended over the entire cluster. These bonding π orbitals make a smaller HOMO-LUMO gap, due to the unlocalized electrons. Examples are clusters $AlBi_3N$ and Al_2BiN that have planar structures with HOMO-LUMO gap of 0.509 and 1.329 eV, respectively. The occupied orbitals of $AlBi_3N$ (Fig. 8) have bonding π orbitals extended over all atoms (considering both HOMO), but in Al_2BiN (Fig. 9) the HOMO has bonding π orbitals over Bi atoms,

with a lone p orbital at the N. Similarly the LUMO shows a lone p orbital in one Bi and a bonding π orbital over all the other atoms, this may explain its greater gap.

Clusters with gaps in the visible and UV are mainly the pure bismuth clusters Bi_x and the binary Bi_yN_z. Figure 7 show that binaries Bi_yN_z have the biggest gaps. Various Bi_yN_z structures are similar to the sodium azide; in Figure 10a we show the HOMO and LUMO orbitals for BiN_3. The HOMOα is a bonding π orbital extended over two N atoms and lone p orbitals over all the other atoms; HOMOβ is a bonding π orbital over the Bi
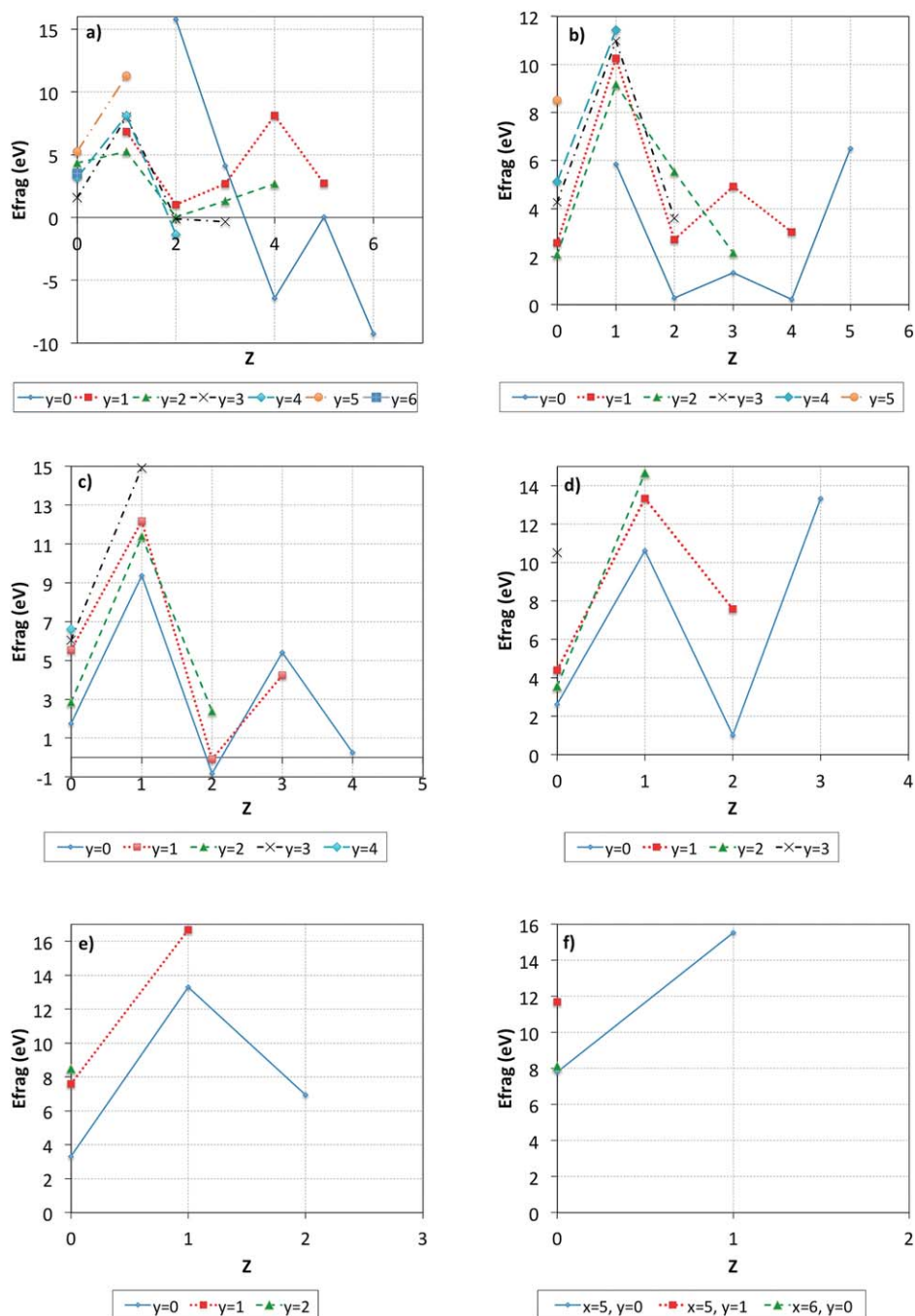
Figure 12. Fragmentation energy as a function of nitrogen concentration for $Al_xBi_yN_z$. a) Without Al ($x = 0$), b) aluminum concentration=1 ($x = 1$), c) aluminum concentration=2 ($x = 2$), d) aluminum concentration=3 ($x = 3$), e) aluminum concentration=4 ($x = 4$), and e) aluminum concentration=5 and 6 ($x = 5$ and $x = 6$). [Color figure can be viewed in the online issue, which is available at wileyonlinelibrary.com.]

and one N, and the LUMOs present many lone p and anti-bonding π orbitals, so we can expect stability in these clusters. BiN_4 shows a similar behavior (Fig. 10b) the HOMOβ is a bonding π orbital between the Bi and the isolated N and antibonding π. The HOMOα has a lone p orbital and an antibonding π.

High multiplicity clusters

Other interesting aspect are their magnetic properties, all the odd clusters are open shell systems with a small magnetic

moment. The multiplicities for the ground state of each cluster are shown in Figures 1–6. Several clusters have higher multiplicity (triplet and quadruplet). High multiplicity states appear mostly in binary clusters that have aluminum or bismuth and nitrogen atoms but not in ternaries (Al_2BiN, $AlBi_2N_2$ are the exceptions). The Bi_3 shows a quadruplet state, this explains the experimental magnetic moment observed.[13] In agreement with our results the measured magnetic moment of the Bi_3 is greater than that obtained for Bi_5 that is a doublet.

Table 4. Fragmentation energies E_{frag} (eV) of $Al_xBi_yN_z$ clusters.		
Cluster	Fragments	E_{frag} (eV)
N2	2(N)	15.771
N3	N2+N	4.126
N4	2(N2)	−6.402
N5	N2+N3	0.034
N6	3(N2)	−9.246
Bi1N1	Bi+N	6.833
Bi1N2	Bi+N2	1.023
Bi1N3	Bi+N3	2.669
Bi1N4	Bi+N3+N	8.140
Bi1N5	Bi+N3+N2	2.732
Bi2	Bi+Bi	4.361
Bi2N1	Bi2+N	5.241
Bi2N2	Bi2+N2	0.027
Bi2N3	Bi2+N3	1.341
Bi2N4	Bi2N+N3	2.679
Bi3	Bi2+Bi	1.590
Bi3N1	Bi3+N	8.002
Bi3N2	Bi3+N2	−0.118
Bi3N3	Bi3+N3	−0.339
Bi4	2(Bi2)	3.177
Bi4N1	2(Bi2)+N	8.105
Bi4N2	Bi4+N2	−1.352
Bi5	2(Bi2)+Bi	5.236
Bi5N1	2(Bi2)+Bi+N	11.294
Bi6	3(Bi2)	3.528
Al1N1	Al+N	5.857
Al1N2	Al+N2	0.279
Al1N3	Al+N3	1.332
Al1N4	AlN2+N2	0.220
Al1N5	Al+2(N2)+N	6.503
Al1Bi1	Al+Bi	2.566
Al1Bi1N1	Al+Bi+N	10.245
Al1Bi1N2	Al+Bi+N2	2.710
Al1Bi1N3	Al+Bi+N3	4.929
Al1Bi1N4	Al+Bi+2(N2)	3.031
Al1Bi2	Al+Bi2	2.070
Al1Bi2N1	Al+Bi2+N	9.157
Al1Bi2N2	Al+2(Bi)+N2	5.540
Al1Bi2N3	Al+Bi2+N3	2.160
Al1Bi3	Al+Bi3	4.271
Al1Bi3N1	Al+Bi3+N	10.980
Al1Bi3N2	Al+Bi2+Bi+N2	3.595
Al1Bi4	Al+2(Bi2)	5.113
Al1Bi4N1	Al+2(Bi2)+N	11.434
Al1Bi5	Al+2(Bi2)+Bi	8.522
Al2	2(Al)	1.742
Al2N1	Al2+N	9.363
Al2N2	Al2+N2	−0.827
Al2N3	2(Al)+N3	5.411
Al2N4	Al2+2(N2)	0.262
Al2Bi1	2(Al)+Bi	5.535
Al2Bi1N1	Al2+Bi+N	12.188
Al2Bi1N2	Al2Bi+N2	−0.091
Al2Bi1N3	Al2Bi+N3	4.244
Al2Bi2	Al2+Bi2	2.848
Al2Bi2N1	Al2+Bi2+N	11.392
Al2Bi2N2	Al2+Bi2+N2	2.388
Al2Bi3	Al2+Bi3	6.052
Al2Bi3N1	Al2+Bi2+Bi+N	14.905
Al2Bi4	Al2+2(Bi2)	6.596
Al3	Al2+Al	2.634
Al3N1	Al3+N	10.606
Al3N2	Al3+N2	1.007
Al3N3	Al2+Al+N2+N	13.340
Al3Bi1	Al3+Bi	4.401
Al3Bi1N1	Al3+Bi+N	13.335

TABLE 4. Continued		
Cluster	Fragments	E_{frag} (eV)
Al3Bi1N2	Al2+Al+Bi+N2	7.579
Al3Bi2	Al3+Bi2	3.565
Al3Bi2N1	Al2+Al+Bi2+N	14.667
Al3Bi3	Al2+Al+Bi2+Bi	10.530
Al4	2(Al2)	3.318
Al4N1	2(Al2)+N	13.300
Al4N2	2(Al2)+N2	6.940
Al4Bi1	2(Al2)+Bi	7.578
Al4Bi1N1	2(Al2)+Bi+N	16.671
Al4Bi2	2(Al2)+Bi2	8.483
Al5	2(Al2)+Al	7.802
Al5N1	2(Al2)+Al+N	15.535
Al5Bi1	2(Al2)+Al+Bi	11.681
Al6	3(Al2)	8.106

Aluminum clusters $Al_{n=2,4,6}$ show high multiplicities (triplets) as observed previously by Stern-Gerlach experiments.[1] These experiments show that even clusters Al_4, Al_6, and Al_8 have greater magnetic deflections compared with the odd clusters Al_3 and Al_7. There is a tendency of small clusters to show high multiplicity states; also the magnetic response decreases with the clusters size. All high multiplicity clusters have errors below 3% in the $<S^2>$ value compared with exact eigenvalue, ensuring no spin-contamination problems.

Overall, high multiplicity clusters contain aluminum or bismuth atoms but not both, as shown by the triplets Al_5N, Al_2N_2, AlN, Bi_4N_2, BiN_5, and BiN_3 and quadruplet BiN_2. Important exceptions are quadruplet $AlBi_2N_2$ and triplet Al_2BiN. Bismuth and aluminum atoms tend to promote high multiplicity states in small clusters.

Odd-atom clusters show a particular behavior in the HOMO-LUMO gap (Fig. 7). Clusters with doublet multiplicity show a small gap in the range 0.338–1.986 eV compared to the odd-atom clusters with quadruplet multiplicity in the range of 0.765–3.537 eV. This is consistent with the odd–even oscillation in the HOMO-LUMO gaps that explains the small gap in doublet odd-atom clusters but showing an increase in the gap for quadruplet odd-atom clusters.
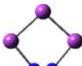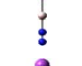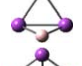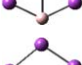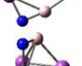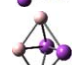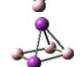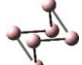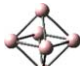
Fragmentation and formation energies

To analyze the stability of the obtained clusters we started calculating the formation energy per atom as

Table 5. NICS (ppm) for planar $Al_xBi_yN_z$ clusters.			
Cluster	NICS (ppm)	Cluster	NICS (ppm)
Al2N2	−31.350	Al2Bi1	−6.429
Bi3N2	−10.831	Al1N5	−15.453
Al2N4	−19.272	Al4N2	−24.769
Al3N2	−38.648	Al3Bi1N2	−4.350
Al1Bi2	7.493	Al5	−14.988
Al2Bi2N2	−7.435	Al1Bi2N1	−9.134
Al3	−36.863	Al2Bi1N1	−30.922
Al4	−35.831	Al3Bi1N1	−22.851
Al3Bi1	−27.495	Al5N1	−15.368
Bi2N1	−12.641	Al4Bi1N1	−5.292
Al2N3	−3.595		

Table 6. Total energies E_T, energy differences ΔE between the two geometries nearest in energy with and without zero point energy correction, all energies in eV, point group symmetry (Symm) and Geometries. [Color table can be viewed in the online issue, which is available at wileyonlinelibrary.com.]

Clusters	M	E_T (eV)	ΔE (eV)	$E_T + ZPE$ (eV)	ΔE (eV)	Symm	Geometry
Bi3N2	2	−3425.491	0.000	−3425.307	0.000	C_{2v}	
	2	−3425.440	0.050	−3425.254	0.053	C_s	
Al1Bi1N2	1	−9724.569	0.000	−9724.433	0.000	C_s	
	1	−9724.557	0.012	−9724.414	0.019	$C\infty v$	
Al1Bi3	1	−7043.439	0.000	−7043.430	0.000	C_s	
	1	−7043.406	0.032	−7043.393	0.037	C_{2v}	
Al1Bi3N1	2	−8532.786	0.000	−8532.698	0.000	C_s	
	2	−8532.739	0.047	−8532.659	0.039	C_1	
Al3Bi2	2	−20088.531	0.000	−20088.571	0.000	C_s	
	2	−20088.486	0.045	−20088.526	0.044	C_1	
Al6	1	−39581.276	0.000	−39581.094	0.000	D_{3d}	
	3	−39581.268	0.008	−39581.103	−0.009	D_{2h}	

$$E_{form} = (xE_{Al} + yE_{Bi} + zE_N - E_{Al_xBi_yN_z})/(x+y+z) \qquad (2)$$

where E_{Al}, E_{Bi}, and E_N are the ground state energy of the referred atom, and $E_{AlxBiyNz}$ is the total energy of the $Al_xBi_yN_z$ cluster. Positive formation energy indicates stability of the cluster with respect to the atomic components. Figure 11 shows the formation energy per atom for all the studied clusters as a function of N concentration for different Al concentrations. All of them show an increase as the nitrogen concentration increases, except for the case of pure N in Figure 11a. Most of the clusters with high formation energies have nitrogen atoms. N_3 and N_2 have the highest formation energies 6.632 and 7.886 eV/atom, respectively. Clusters that contain nitrogen Al_x-Bi_yN_z, Bi_yN_z, and Al_xN_z show high formation energies.

Clusters without nitrogen show low formation energy, the pure clusters Bi_x, Al_x, and the binary of these Al_xBi_y have formation energies in ranges of: 1.984–2.975, 0.871–2.257, and 1.283–2.874 eV/atom, respectively. Al_xN_z clusters show high formation energies and various stable clusters.[21]

The obtained geometries suggest that most of those having N2 or N3, may fragment. To see if this would happen, we calculated the fragmentation energy defined as the energy difference between the cluster and a sum of various stable fragments (atoms, dimmers, and trimers).

$$E_{Frag} = \sum_i E_{fragmente(i)} - E_{Al_xBi_yN_z} \qquad (3)$$

The choice of a combination of fragments considered the geometry of the cluster and the relative stability between the possible fragments. According with our definition, negative fragmentation energy indicates a tendency to a spontaneous fragmentation or that it will be difficult synthesis, and a positive energy is the tendency to keep the cluster together. It should be taken in account that our calculations do not include the dynamics. The fragmentation energies were calculated for all combinations and we report only those with the smallest E_{frag}. In Figure 12 the fragmentation energies as a function of N concentration are shown. The fragments are given in Table 4. In general low N concentration increases the stability of the cluster. In fact, clusters with one nitrogen have the highest E_{frag}, while, clusters with even number of nitrogen have the lowest E_{frag}.

The more unstable clusters are N_4, N_6, Al_2N_2, and Bi_3N_2. Their low fragmentation energies are due to nitrogen dimers

and agree well with other works.[43,44] Overall, ternary clusters $Al_xBi_yN_z$ have the highest fragmentation energies in the range of 2.388–16.671 eV, followed by nitrogen clusters with an extremely wide range that goes from 0.034–15.771 eV. Binaries Al_xN_z and Bi_yN_z have ranges of 0.262–15.535 and 0.027–11.294 eV, respectively. The lowest fragmentation energies correspond to Al_2N_4 and Bi_2N_2 showing a tendency to form nitrogen dimers; conversely, highest values correspond to Al_5N and Al_5Bi. Clusters without nitrogen, as the binaries Al_xBi_y show smaller ranges 2.070–11.681 eV. Many of these clusters can be considered stable in agreement with experiments.[27]

Fragmentation energies also show odd–even oscillation similar to the HOMO-LUMO gap. Even-atom clusters have higher fragmentation energies compared to the odd-atom clusters in the same series. This is in agreement with a bigger HOMO-LUMO gap associated to a more stable form.

All clusters with negative or near zero fragmentation energy have two or four nitrogens. In most of them the N are forming N_2 with a small interaction with Bi or Al and thus one of the fragments would be a nitrogen molecule. In the clusters with positive fragmentation energy that have N_2 as a fragment, the interaction between the metal and the nitrogen atoms is stronger (the nitrogen-metal bond is shorter) and thus they will not fragment.

We have calculated (at the same level of theory) the nuclear independent chemical shifts (NICS) for planar rings, shown in Table 5. Negative NICS value indicates an aromatic character and positive NiCS an antiaromatic character. Most planar clusters show negative NICS and positive fragmentation energy. This indicates that the planar geometry is stable due to the aromatic energy. Al_2N_2 and Bi_3N_2 have negative NICS and negative fragmentation energy. The N_2 bond is too strong.

Conversely, the Jellium model predicts the stabilization by the number of valence electrons. Considering the 2D Jellium model[45,46] we find Al_4, Al_5N, and Al_3BiN_2 with 12, 20, and 24 electrons, respectively, they have a closed shell and should be stable. Taking three effective electrons for Bi (by the inert pair effect) Al_3Bi and Al_4BiN have 12 and 20 effective electrons which is consistent with the 2D Jellium and should also be stable as also indicated by E_{frag} and E_{form}. The 3D Jellium model predicts[47] that Bi_3N, Bi_2N_2, Al_5Bi, N_4, and BiN_3 are stable, but it is experimentally known that N_4 breaks into nitrogen dimers. Finally, Al_3Bi_2N, Al_2Bi_3N, $AlBi_4N$, and Bi_5N with 20 effective electrons are stable. In general, NICS, E_{frag}, and the Jellium model agree except in those cases where we have an even number of nitrogen atoms. This is due to high bonding energy of the N_2 molecule.

Geometries with small energy differences

Search of global minima for each stoichiometry requires energy differences between configurations to be bigger than the accuracy of the DFT methods. Energy differences ΔE above 0.05 eV are considered over the error. We considered that the geometries found are more stable if the energy difference, ΔE, with the next minimum energy is above this range. Table 6

shows geometries where differences with global minimum are below 0.05 eV.

In the case of Al_6, the energy difference between structures is so small that it is necessary to include the zero point energy to be in agreement with the experimental results.[1] It is important to mention that also in this case the two minimum energy states have different multiplicity.

Conclusions

DFT calculations have been carried out on $Al_xBi_yN_z$ clusters with $x + y + z < 7$. Binary cluster's properties can be understood from its constituent atoms. Similarly to Al_x, Al_xN_z clusters have small gaps and planar structures, with low fragmentation energies, high formation energies, and some have high multiplicity states. Bi_nN_m clusters have wide HOMO-LUMO gaps in the visible and UV range, they are similar to other metal-azides. Binaries Al_xBi_y that have a HOMO-LUMO gap around 1 eV are considered stable with low fragmentation energies, most forming 3D structures with low multiplicity. Ternary compounds have planar and 3D structures depending on which is the most abundant atom, Al or Bi. High multiplicity states are also present in $Al_xBi_yN_z$ clusters; they have small gaps. They have high fragmentation energies and π bonds that make them very stable. In all these compounds, the bonding has a π character. The nitrogen content increases the formation energy but the tendencies to form N dimers lower their stability and they are easily fragmented. Most planar structures have an aromatic character.

[1] D. M. Cox, D. J. Trevor, R. L. Whetten, E. A. Rohlfing, A. Kaldor, *J. Chem. Phys.* **1986**, *84*, 4651.

[2] L. Hanley, S. L. Anderson, *Chem. Phys. Lett.* **1986**, *129*, 429.

[3] X. Li, H. Wu, X. B. Wang, L. S. Wang, *Phys. Rev. Lett.* **1998**, *81*, 1909.

[4] R. O. Jones, *J. Chem. Phys.* **1993**, *99*, 1194.

[5] P. Jena, *J. Phys. Chem. Lett.* **2013**, *4*, 1432.

[6] N. Debrov, R. Ahlrichs, *J. Chem. Phys.* **2010**, *132*, 164703.

[7] J. S. Thayer, *J. Chem. Educ.* **2005**, *82*, 1721.

[8] X. Gonze, J. P. Michenaud, J. P. Vigneron, *Phys. Scr.* **1988**, *37*, 785.

[9] M. G. Mitch, S. J. Chase, J. Fortner, R. Q. Yu, J. S. Lannin, *Phys. Rev. Lett.* **1991**, *67*, 875.

[10] M. E. Geusic, R. R. Freeman, M. A. Duncan, *J. Chem. Phys.* **1988**, *89*, 223.

[11] H. K. Yuan, H. Chen, A. L. Kuang, Y. Miao, Z. H. Xiong, *J. Chem. Phys.* **2008**, *128*, 094305.

[12] R. Kelting, A. Baldes, U. Schwarz, T. Rapps, D. Schooss, P. Weis, C. Neiss, F. Weigend, M. M. Kappes, *J. Chem. Phys.* **2012**, *136*, 154309.

[13] S. Yin, X. Xu, R. Moro, W. A. de Heer, *Phys. Rev. B* **2005**, *72*, 174410.

[14] M. H. Mikkelä, M. Tchaplyguine, S. Urpelainen, K. Jänkälä, O. Björneholm, M. Huttula, *J. Appl. Phys.* **2012** *112*, 084326.

[15] S. Bräse, C. Gil, K. Knepper, V. Zimmermann, *Angew. Chem. Int. Ed.* **2005**, *44*, 5188.

[16] B. P. Aduev, E. D. Aluker, G. M. Belokurov, Y. A. Zakharov, A. G. Krechetov, *J. Exp. Theor. Phys.* **1999**, *89*, 906.

[17] K. O. Christe, W. W. Wilson, J. A. Sheehy, J. A. Boatz, *Angew. Chem. Int. Ed.* **1999**, *38*, 2004.

[18] X. Wang, H. Hu, A. Tian, N. B. Wong, S. Chien, W. Li, *Chem. Phys. Lett.* **2000**, *329*, 483.

[19] A. Vij, J. G. Pavlovich, W. W. Wilson, K. O. Christe, *Angew. Chem. Int. Ed.* **2002**, *41*, 3051.

[20] I. Vurgaftman, J. R. Meyer, L. R. Ram-Mohan, *J. Appl. Phys.* **2001**, *89*, 5815.

[21] L. Guo, H. S. Wu, Z. H. Jin, *Int. J. Quantum Chem.* **2005**, *103*, 291.

[22] V. F. Curotto, R. P. Diez, *Comput. Mater. Sci.* **2011**, *50*, 3390.

[23] B. B. Averkiev, A. I. Boldyreva, *J. Chem. Phys.* **2006** *125*, 124305.

[24] S. K. Nayak, S. N. Khanna, P. Jena, *Phys. Rev. B* **1998**, *57*, 3787.

[25] N. R. Panyala, V. Prysiazhnyi, P. Slavíček, M. Černák, J. Havel, *Rapid Commun. Mass Spectrom.* **2011**, *25*, 1687.

[26] C. E. Jones, Jr., P. A. Clayborne, J. U. Reveles, J. J. Melko, U. Gupta, S. N. Khanna, A. W. Castleman, *J. Phys. Chem. A* **2008**, *112*, 13316.

[27] Z. Sun, Q. Zhu, Z. Gao, Z. Tang, *Rapid. Commun. Mass Spectrom.* **2009**, *23*, 2663.

[28] A. Villinger, A. Schulz, *Angew. Chem. Int. Ed.* **2010**, *49*, 8017.

[29] K. Rosenstengel, A. Schulz, A. Villinger, *Inorg. Chem.* **2013**, *52*, 6110.

[30] S. Heiles, R. L. Johnston, *Int. J. Quantum Chem.* **2013**, *113*, 2091.

[31] A. Zhigljavsky, and A. Žilinskas, Stochastic Global Optimization; Springer-Verlag: Berlin, **2008**; pp. 29-90.

[32] M. J. Frisch, G. W. Trucks, H. B. Schlegel, G. E. Scuseria, M. A. Robb, J. R. Cheeseman, G. Scalmani, V. Barone, B. Mennucci, G. A. Petersson, H. Nakatsuji, M. Caricato, X. Li, H. P. Hratchian, A. F. Izmaylov, J. Bloino, G. Zheng, J. L. Sonnenberg, M. Hada, M. Ehara, K. Toyota, R. Fukuda, J. Hasegawa, M. Ishida, T. Nakajima, Y. Honda, O. Kitao, H. Nakai, T. Vreven, J. A. Montgomery, Jr., J. E. Peralta, F. Ogliaro, M. Bearpark, J. J. Heyd, E. Brothers, K. N. Kudin, V. N. Staroverov, R. Kobayashi, J. Normand, K. Raghavachari, A. Rendell, J. C. Burant, S. S. Iyengar, J. Tomasi, M. Cossi, N. Rega, J. M. Millam, M. Klene, J. E. Knox, J. B. V. Cross, C. Bakken, C. Adamo, J. Jaramillo, R. Gomperts, R. E. Stratmann, O. Yazyev, A. J. Austin, R. Cammi, C. Pomelli, J. W. Ochterski, R. L. Martin, K. Morokuma, V. G. Zakrzewski, G. A. Voth, P. Salvador, J. J. Dannenberg, S. Dapprich, A. D. Daniels, O. Farkas, J. B. Foresman, J. V. Ortiz, J. Cioslowski, D. J. Fox, Gaussian 09, Revision A.02; Gaussian, Inc.: Wallingford, CT, **2009**.

[33] Y. Zhao, D. G. Truhlar, *J. Chem. Phys.* **2006**, *125*, 194101.

[34] T. Clark, J. Chandrasekhar, G. W. Spitznagel, P. von R. Schleyer, *J. Comput Chem.* **1983**, *4*, 294.

[35] P. M. W. Gill, B. G. Johnson, J. A. Pople, M. J. Frisch, *Chem. Phys. Lett.* **1992**, *197*, 499.

[36] C. Effantin, A. Topouzkhanian, J. Figuet, J. d'Incan, R. F. Barrow, J. Verges, *J. Phys. B: At. Mol. Phys.* **1982**, *15*, 3829.

[37] L. S. Wang, Y. T. Lee, D. A. Shirley, K. Balasubramanian, P. Feng, *J. Chem. Phys.* **1990**, *93*, 6310.

[38] L. Guo, *J. Mol. Struct.* **2007**, *809*, 181.

[39] L. Guo, H. S. Wu, *Solid State Ionics*, **2006**, *177*, 437.

[40] S. T. Sun, H. T. Liu, Z. C. Tang, *J. Phys. Chem. A* **2006**, *110*, 5004.

[41] D. R. Lide, CRC Handbook of Chemistry and Physics, 82nd ed.; CRC Press: Boca Raton, **2001**.

[42] K. P. Huber, G. Herzberg, Molecular Spectra and Molecular Structure. IV. Constants of Diatomic Molecules; Van Nostrand Reinhold Co: New York, **1979**.

[43] L. Candido, J. N. Teixeira, J. L. F. Da Silva, G. Q. Hai, *Phys. Rev. B* **2012**, *85*, 245404.

[44] F. Cacace, G. de Petris, A. Troiani, *Science*, **2002**, *295*, 480.

[45] S. M. Reimann, et al., *Phys. Rev. B* **1997**, *56*, 147.

[46] E. Janssens, H. Tanaka, S. Neukermans, R. E Silverans, P. Lievens, *New J. Phys.* **2003**, *5*, 46.

[47] M. Koskinen, P. O. Lipas, M. Manninen, *Z. Phys. D* **1995** *35*, 285.